

# MANual vs. automatIc local activation time annotation for guiding Premature Ventricular Complex ablation procedures (MANIaC-PVC study)

Beatriz Jáuregui<sup>1</sup>, Juan Fernández-Armenta<sup>2</sup>, Juan Acosta<sup>3</sup>, Diego Penela<sup>1,4</sup>, Cheryl Terés<sup>1</sup>, Augusto Ordóñez<sup>1</sup>, David Soto-Iglesias<sup>1</sup>, Etelvino Silva<sup>2</sup>, Alfredo Chauca<sup>1</sup>, José M. Carreño<sup>1</sup>, Claudia Scherer<sup>1</sup>, Alonso Pedrote<sup>3</sup> and Antonio Berruezo<sup>1\*</sup>

<sup>1</sup>Heart Institute, Teknon Medical Center, C/Vilana, 12, 08022 Barcelona, Spain; <sup>2</sup>Puerta del Mar University Hospital, Cádiz, Spain; <sup>3</sup>Virgen del Rocío University Hospital, Sevilla, Spain; and <sup>4</sup>Ospedale Guglielmo da Saliceto, Piacenza, Italy

Received 9 December 2020; editorial decision 13 March 2021; accepted after revision 17 March 2021

## Aims

To assess potential benefits of a local activation time (LAT) automatic acquisition protocol using wavefront annotation plus an ECG pattern matching algorithm [automatic (AUT)-arm] during premature ventricular complex (PVC) ablation procedures.

## Methods and results

Prospective, randomized, controlled, and international multicentre study (NCT03340922). One hundred consecutive patients with indication for PVC ablation were enrolled and randomized to AUT ( $n=50$ ) or manual (MAN,  $n=50$ ) annotation protocols using the CARTO3 navigation system. The primary endpoint was mapping success. Clinical success was defined as a PVC-burden reduction of  $\geq 80\%$  in the 24-h Holter within 6 months after the procedure. Mean age was  $56 \pm 14$  years, 54% men. The mean baseline PVC burden was  $25 \pm 13\%$ , and mean left ventricular ejection fraction (LVEF)  $55 \pm 11\%$ . Baseline characteristics were similar between the groups. The most frequent PVC-site of origin were right ventricular outflow tract (41%), LV (25%), and left ventricular outflow tract (17%), without differences between groups. Radiofrequency (RF) time and number of RF applications were similar for both groups. Mapping and procedure times were significantly shorter in the AUT-arm ( $25.5 \pm 14.3$  vs.  $32.8 \pm 12.6$  min,  $P=0.009$ ; and  $54.8 \pm 24.8$  vs.  $67.4 \pm 25.2$ ,  $P=0.014$ , respectively), while more mapping points were acquired [ $136$  (94–222) AUT vs.  $79$  (52–111) MAN;  $P<0.001$ ]. Mapping and clinical success were similar in both groups. There were no procedure-related complications.

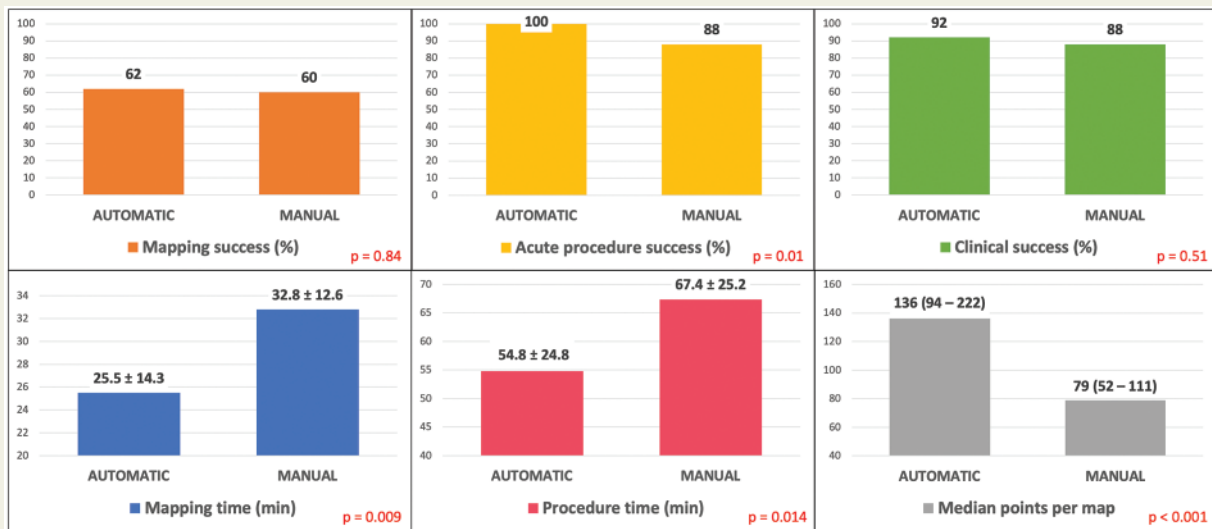
## Conclusion

The use of a complete automatic protocol for LAT annotation during PVC ablation procedures allows to achieve similar clinical endpoints with higher procedural efficiency when compared with conventional, manual annotation carried out by expert operators.

\* Corresponding author. Tel: +34 932 90 62 00; fax: +34 932 11 26 90. E-mail address: antonio.berruezo@quironsalud.es

Published on behalf of the European Society of Cardiology. All rights reserved. © The Author(s) 2021. For permissions, please email: journals.permissions@oup.com.

## Graphical Abstract



## Keywords

Premature ventricular complexes • Catheter ablation • Local activation time • Automatic annotation • Wavefront • Activation mapping

## What's new?

- A fully automatic acquisition of electroanatomical maps (EAM) during premature ventricular complex (PVC) ablation procedures is feasible, using wavefront for local activation time (LAT) annotation and an ECG pattern matching algorithm to precisely identify the clinical PVC.
- Compared with manual activation mapping carried out by expert operators, this automatic approach accurately identifies the ablation target point, reaching similar clinical outcomes.
- The automatic acquisition of EAM during PVC ablation procedures permits to improve procedures' efficiency in terms of mapping time, procedure time, and density of the acquired maps.

## Introduction

Catheter ablation is an accepted and effective treatment strategy for management of premature ventricular complexes (PVCs).<sup>1</sup> Conventional PVC mapping requires experience performing real-time interpretation of local signals and annotating the local activation time (LAT) in unipolar (U-EGM) and/or bipolar electrograms (B-EGM). However, the major disadvantages of U-EGMs are susceptibility to noise and the presence of substantial far-field signal,<sup>2</sup> which limit their routine use during activation mapping for some substrates. Drawbacks to B-EGMs include being influenced by wavefront (WF) direction, bipole orientation, electrode size, and inter-electrode

spacing.<sup>3</sup> Furthermore, LAT assessment on B-EGMs is often challenging, especially in cases with low-voltage EGMs with multiple components. Recently, El Haddad et al.<sup>4</sup> described an automated algorithm that detects the maximal  $-dV/dt$  in the U-EGM within the window demarcated by the B-EGM that achieved the highest accuracy in algorithmic mapping of atrial and ventricular tachycardia. A recent study<sup>5</sup> showed a good correlation between manual and automatic LAT annotation systems. However, data about its utility, accuracy in PVC ablation procedures, and its clinical impact are scarce.

The present randomized study aims to analyse the accuracy of this novel algorithmic method (Wavefront, CARTO3<sup>®</sup>, Biosense Webster, Diamond Bar, CA, USA) together with the use of an automatic ECG pattern recognition algorithm, by comparison with conventional manual annotation and visual PVC-ECG recognition in a multicentre cohort of patients referred for PVC ablation.

## Methods

### Patient sample and randomization

This is a prospective, randomized, controlled, and international multicentre study (NCT03340922), including 100 consecutive patients referred for a first PVC ablation. One hundred and fifty consecutive patients were initially recruited in four centres. Forty patients (27%) had to be excluded due to a very low burden of PVCs (<1 PVC/min)<sup>6</sup> during cardiac monitoring before the procedure, being targeted by pace-mapping. Nine patients (6%) could not be ablated due to complete absence of PVCs. One patient was not ablated after documenting a para-Hisian SOO. Finally, 100 patients were included for analysis. All patients were

randomized on a 1:1 basis to each of the LAT annotation methods before the ablation procedure: (i) AUT-method, using WF annotation plus an automatic ECG pattern recognition algorithm and (ii) manual (MAN)-method, using real-time manual annotation by an expert operator (cardiac electrophysiologist with at least 5-year experience), plus visual inspection of the ECG to acquire points whenever the PVC of interest is observed (Figure 1).

Age <18 years, repeated procedures, a low burden of PVCs during the procedure (< 1 PVC per minute),<sup>6</sup> pregnancy, presence of concomitant investigation treatments, or patient's refusal to participate in the study, were exclusion criteria. The study complied with the Declaration of Helsinki. The local Ethical Committee approved the study protocol and all included participants signed the informed consent.

## Definitions and endpoints

Mapping success was defined as complete PVC abolition after radiofrequency (RF) applications at the earliest activation site (EAS) identified using the assigned mapping method. A maximum of 2 RF applications with appropriate parameters (as detailed later) during a maximum of 45 s was allowed. Acute procedure success was defined as complete elimination of the PVC at the end of the procedure. A target point for ablation was defined as any suspected PVC-site of origin (SOO), based on the identified EAS, where RF was delivered according to mapping data. The maximum distance between 2 RF applications to be considered as delivered at the same target point was defined as 5 mm.<sup>7</sup> Clinical success was defined as the PVC-burden reduction of  $\geq 80\%$  in a 24-h Holter performed within 6 months after the procedure, since recurrences can be usually detected during this time period.<sup>8</sup>

The primary endpoint was mapping success using the assigned mapping approach, as previously defined. Mapping time, number of mapped chambers and points, number of target points, RF time, number of RF applications, acute procedure success, and clinical success were considered secondary endpoints of the study.

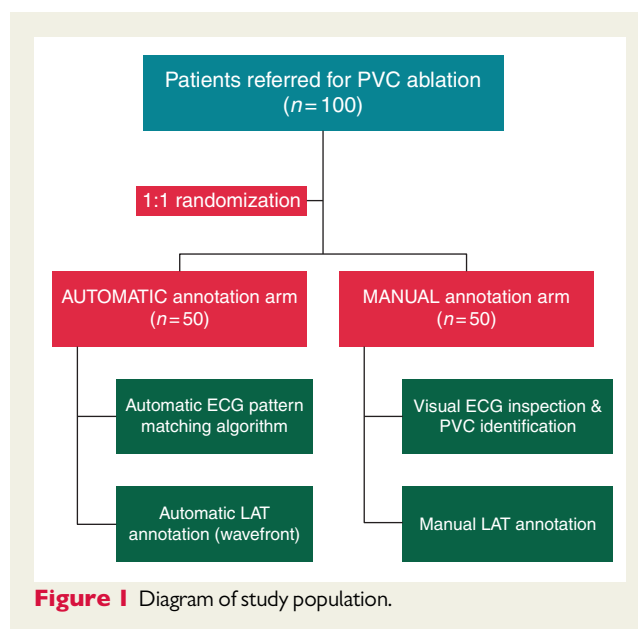
## Activation mapping and annotation methods

Electroanatomical mapping (EAM) was performed using the CARTO3<sup>®</sup> navigation system (Biosense Webster, Irvine, CA, USA) with a 3.5 mm irrigated tip catheter (NaviStar<sup>®</sup> ThermoCool<sup>®</sup> or ThermoCool<sup>®</sup> SmartTouch<sup>®</sup>, Biosense Webster). During the procedure, 12-lead surface ECG and intra-cardiac recordings were displayed by an electrophysiology data acquisition system (Bard LabSystem, CR Bard Inc., Lowell, MA, USA or EP-Tracer, CardioTek, Maastricht, The Netherlands).

A detailed activation map of the cardiac chamber/s suspected to contain the PVC-SOO was performed in all patients. If an outflow tract (OT) origin was suspected, the mapped chamber was selected by a pre-defined algorithm (Figure 2) including a previously described clinical score (1 point for each of the following: hypertension, male gender, age > 50 years) together with ECG criteria.<sup>9</sup> The minimum density of points required to obtain an acceptable map was defined as a fill threshold of  $\leq 6$  mm in the 10 ms isochronal area containing the EAS (area of interest), and  $\leq 10$  mm for the complete map.

An ECG surface lead with a well-defined (not bimodal) R-wave peak (R peak = 0 ms) was used as the reference to perform the activation EAM. For both annotation methods, the end of the window of interest was set at the end of the PVC-QRS to avoid the annotation of atrial far-field signals (in cases with retrograde conduction of the PVC). During activation mapping, points were acquired only after a 2-s period of catheter stability.

Activation mapping of additional anatomical structures was allowed under operator criteria, in cases where the suspected SOO could not be identified at the initially mapped chamber. The EAS was considered to be



located at the point with the earliest LAT relative to the onset of PVC on the 12-lead surface ECG, when activation mapping was concluded.

### Manual annotation (MAN-method)

Manual annotation was performed in real time by an experienced electrophysiologist. Mapping points were acquired under operator's criteria after real-time visual inspection of the PVC-QRS morphology. The LAT of every acquired point was measured from the onset of B-EGM (earliest positive or negative deflection) of the distal bipole of the mapping catheter to the defined reference. The U-EGM was used to identify the real onset of B-EGM (Figure 3).

### Automatic annotation (AUT-method)

The annotation of LAT for each acquired point was automatically performed using the LAT annotation tool integrated into CARTO3<sup>®</sup> system, called WF. It uses the maximum negative slope of the distal U-EGM to set the timing of the mapping annotation, displayed on the corresponding B-EGM. The automatic annotation included the use of an ECG recognition pattern algorithm, which is intended to avoid wrong annotation of ventricular complexes other than the clinical PVC. The minimum percentage of QRS similarity was set at  $\geq 98\%$ . If annotation was misleading due to the presence of atrial far-field signals in the selected window of interest, manual elimination of the acquired point was admitted.

In order to perform a comparative *post hoc* analysis between the activation maps obtained with the AUT- and MAN-methods, all cases were reannotated off-line using the alternative annotation method. Manual reannotation was blinded to the AUT-maps. Examples of AUT- vs. MAN-methods for annotation are shown in Figure 3.

## Premature ventricular complex ablation

The PVC ablation was directed to the EAS identified using the assigned annotation method. The temperature limit was set in all cases at 45°C. Power limit was set according to the anatomical structure containing the PVC-SOO: 40 W for the right ventricular outflow tract (RVOT) and the subvalvular left ventricular outflow tract (LVOT), 40 W in the aortic root, 50 W for the right ventricle, 50 W for the left ventricle, and 30 W in the coronary sinus. Ablation points were always tagged using the VisiTag<sup>®</sup>

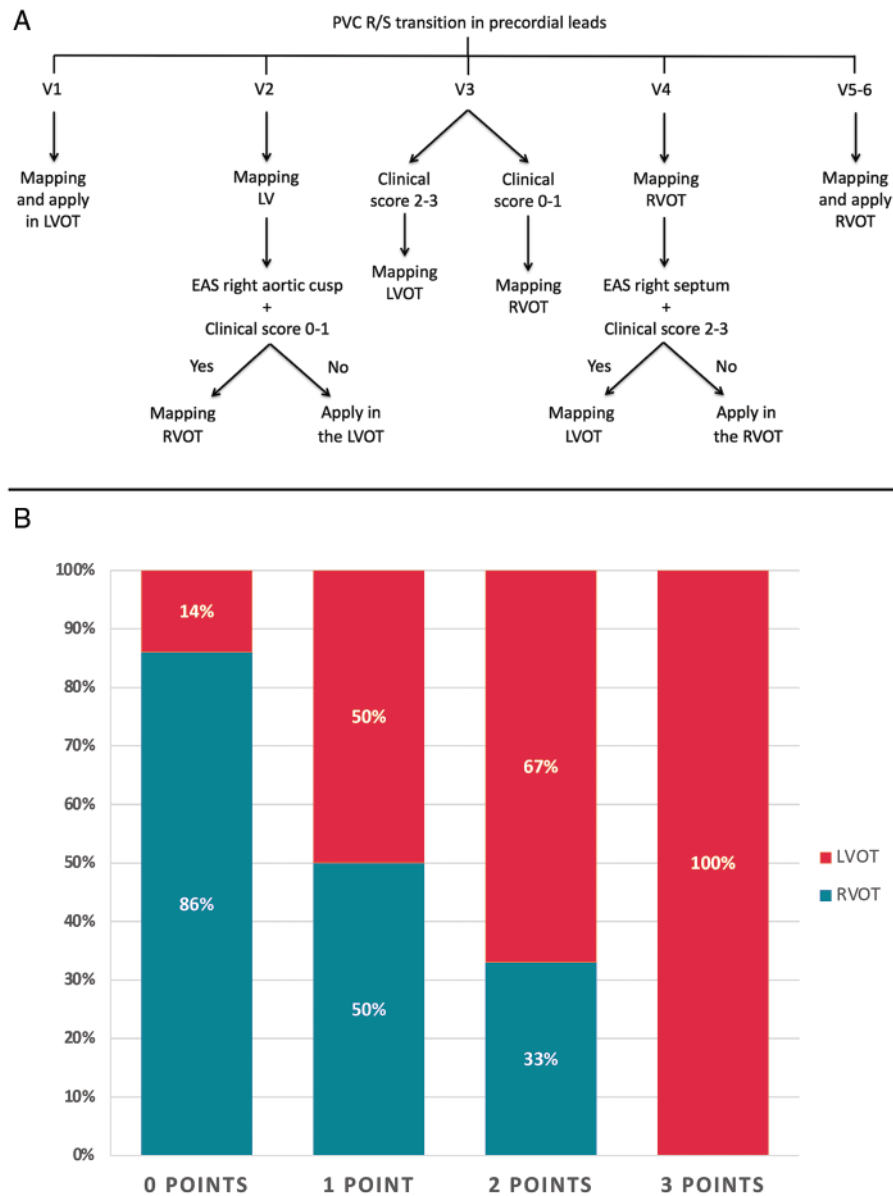


**Figure 2** (A) Algorithm to decide which chamber (RVOT vs. LVOT) to map first in patients with PVCs of OT-suspected origin. (B) Application of a previously described clinical score<sup>9</sup> in OT-PVCs with V3 transition ( $n = 58$ ) to predict the right vs. left SOO and decide the first vascular access. One point is added for each of the following items: hypertension, male gender, and age >50 years. With this approach, 12/18 (67%) patients with V3 transition and a clinical score of 0–1 benefited from a single venous access, or from a single arterial access in 5/7 (71%) with V3 transition and a clinical score of 2–3. LVOT, left ventricular outflow tract; OT, outflow tract; PVC, premature ventricular complex; RVOT, right ventricular outflow tract; SOO, site of origin.

feature included in CARTO3<sup>®</sup>, setting a tag size of 4 mm in diameter. If an RF application was successful, it was maintained for a maximum of 45 s. The point (RFp) at which an RF application was successful to eliminate the PVCs was tagged as the effective RFp (e-RFp). Any additional RF application located within a 5 mm distance from the first application was considered as part of the same target point-suspected SOO. On the contrary, all RF applications located beyond this 5 mm distance were considered as additional target points.

### Clinical follow-up

Clinical follow-up included an outpatient clinic visit one month after ablation procedure. The 12-lead ECG and 24-h ambulatory Holter monitoring were performed. Clinical success was defined as a reduction of  $\geq 80\%$  in the 24-h burden of PVCs within 6 months after ablation, respectively. Antiarrhythmic drugs were routinely discontinued after the procedure, except for those patients needing chronic  $\beta$ -blocker therapy (i.e. those with prior structural heart disease).

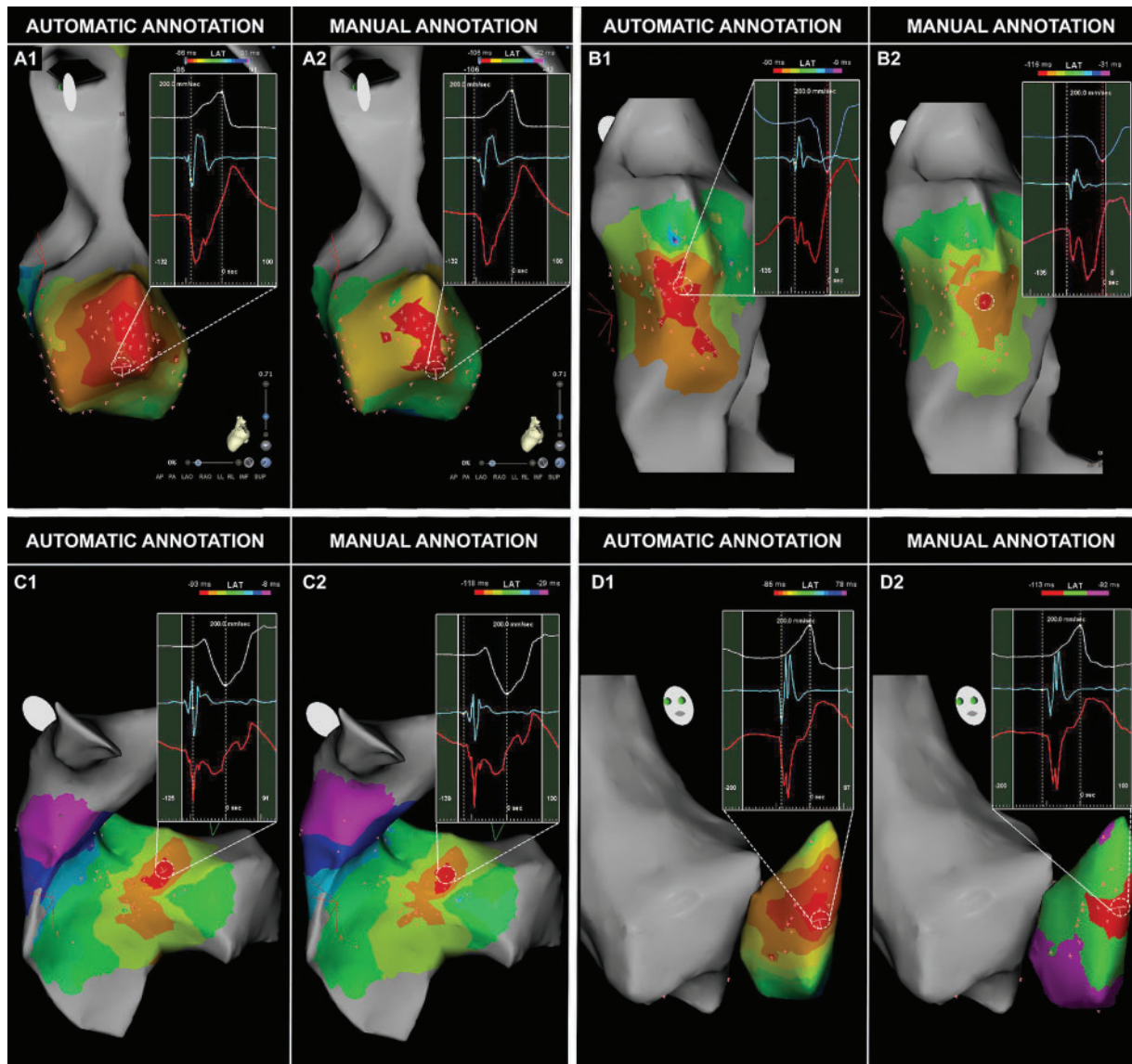


**Figure 3** Several examples of automatic vs. manual annotation approaches. EAM from PVCs arising from LVOT-left coronary cusp (A), lateral RVOT (B), septal tricuspid annulus (C), and LV summit (D) are presented. Blue signals correspond to the B-EGM at the tip of ablation catheter; red signals correspond to the distal U-EGM. Isochronal areas were obtained at 10 ms steps. The EAS is slightly displaced between the annotation approaches in Patients A, B, and D; it is noteworthy, however, that the inter-EAS distance was  $<3$  mm in all cases. For Patient C, the EAS was exactly the same using both annotation systems. B-EGM, bipolar electrogram; EAM, electroanatomical map; EAS, earliest activation site; LVOT, left ventricular outflow tract; PVC, premature ventricular complex; RVOT, right ventricular outflow tract; U-EGM, unipolar electrogram.

### Statistical analysis and sample size calculation

For sample size calculation, a superiority design was assumed. Null hypothesis was considered at the outset that the two annotation methods (MAN- and AUT-methods) are on average equal in terms of mapping success (as previously defined), whereas the alternative hypothesis stated that the proposed annotation methods are not equal. Based on historical controls, the acute mapping success was considered would be 60% for manual annotation, and 85% for automatic annotation using the ECG pattern matching algorithm. The Type I error was set to a value of 5%. The Type II error was set equal to 20%, with a statistical power of 80%. A

sample size of 100 was estimated (50 patients per group). Randomization was performed before ablation using the method of permuted block randomization. The block sizes were randomly chosen as 4 and 6. Continuous variables are presented as mean values  $\pm$  standard deviations, or median [interquartile range (IQR)], as appropriate. Categorical variables are presented as total numbers and percentages. To compare the means of two variables, the Student's *t*-test or Wilcoxon test were used, as needed. Proportions were compared using the  $\chi^2$  or Fisher's exact test, when necessary. For agreement between manual and automatic annotation at the EAS, Bland–Altman analysis was used. A *P*-value  $\leq 0.05$  was considered for statistical significance. Statistics were obtained using

**Table 1** Baseline characteristics

	Total (n = 100)	MAN-method (n = 50)	AUT-method (n = 50)	P-value
Age (years)	56 ± 14	54 ± 15	58 ± 14	0.17
Men (%)	54 (54%)	30 (60%)	24 (48%)	0.23
Hypertension (%)	36 (36%)	15 (30%)	21 (43%)	0.21
Dyslipidaemia (%)	78 (78%)	11 (22%)	11 (22%)	1.0
Diabetes mellitus (%)	9 (9%)	6 (12%)	3 (6%)	0.30
Active smoker (%)	11 (11%)	5 (10%)	6 (12%)	0.75
COPD (%)	3 (3%)	2 (4%)	1 (2%)	0.56
Clinical score <sup>a</sup>	1 (0–2)	1 (0–2)	1 (0–2)	0.98
No SHD	71 (71%)	36 (74%)	35 (70%)	0.57
LVEF (%)	55 ± 11	56 ± 11	55 ± 12	0.67
NYHA class (%)	1 (1–2)	1 (1–2)	1 (1–2)	0.31
Atrial fibrillation (%)	8 (8%)	4 (8%)	4 (8%)	1.0
Conduction disease (%)	14 (14%)	8 (16%)	6 (12%)	0.56
Pacemaker carrier (%)	3 (3%)	1 (2%)	2 (4%)	0.56
Baseline PVC burden (%)	25 ± 13	25 ± 14	25 ± 12	1.0
Sinus rhythm QRS (ms)	92 ± 18	92 ± 17	92 ± 19	1.0
PVC-QRS (ms)	153 ± 28	147 ± 28	158 ± 28	0.05
PVC-LBBB morphology	81 (81%)	39 (80%)	42 (84%)	0.57
PVC coupling (ms)	487 ± 91	482 ± 88	491 ± 94	0.62
Treatment				
β-Blockers	64 (64%)	31 (62%)	33 (66%)	0.68
Amiodarone	8 (8%)	3 (6%)	5 (10%)	0.46
Flecainide	3 (3%)	2 (4%)	1 (2%)	0.56
ACEI/ARB	31 (31%)	13 (26%)	18 (36%)	0.28

COPD, chronic obstructive pulmonary disease; LBBB, left bundle branch block; LVEF, left ventricular ejection fraction; NYHA, New York Heart Association; PVC, premature ventricular complex; SHD, structural heart disease.

<sup>a</sup>Clinical score to predict LVOT origin in PVCs with inferior axis and V3 transition. One point is added for each of the following items: hypertension, male gender, age >50 years. The mean predicted LVOT probability is 15% for score 0, 26% for score 1, 60% for score 2, and 87% for score 3.<sup>9</sup>

IBM SPSS Statistics, version 26.0 (IBM Corp. Released 2019; IBM Corp., Armonk, NY, USA).

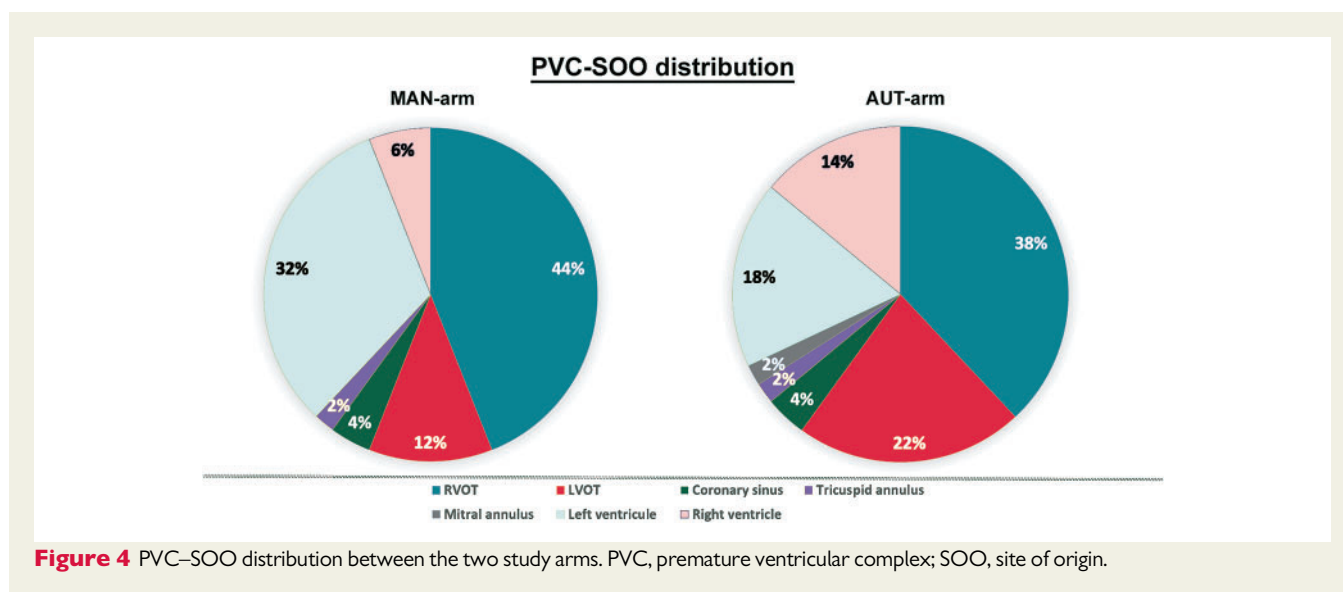
## Results

Mean age was 56 ± 14 years, 54% men. The mean left ventricular ejection fraction (LVEF) was 55 ± 11%. Twenty-eight patients (28%) had a previously diagnosed structural heart disease; from them, 18/28 (64%) had a non-ischaemic cardiomyopathy with a mean LVEF of 42 ± 6%. Mean NYHA class was 1.9 ± 0.6 points, and mean baseline PVC burden was 25 ± 13%. Baseline characteristics were similar between both study arms and are summarized in Table 1. The most frequent PVC-SOO were RVOT (41%), LV (25%), and LVOT (17%), with no MAN vs. AUT global differences ( $P=0.40$ ), and similar proportions of OT- (56% MAN vs. 60% AUT;  $P=0.69$ ) and RVOT-SOO (44% MAN vs. 38% AUT;  $P=0.54$ , Figure 4). Out of 58 cases with an OT origin, 25 (43%) showed a PVC-QRS with V3 transition; for them, the use of a previously described clinical score<sup>9</sup> was used to decide which chamber to map first (Figure 2). In 11/25 (44%) of the cases with an LV origin the SOO was located at the LV summit.

## Mapping comparison between MAN- and AUT-methods

The propagation pattern, measured as 10 ms isochronal area, was similar between the groups (1.29 ± 2.17 cm<sup>2</sup> AUT vs. 1.74 ± 2.28 cm<sup>2</sup> MAN;  $P=0.14$ ). With regards to the EAS annotation, there was a significant good correlation in LAT between the AUT and MAN maps ( $r=0.84$ ,  $P<0.001$ ; Figure 5A). Further on, and in line with previous reports,<sup>5</sup> there was a systematic delayed detection of LAT at the EAS in the AUT-arm (mean 22.36 ± 13.19 ms, Figure 5B), especially in left-sided PVCs (27.94 ± 11.46 ms for left-sided vs. 17.49 ± 12.78 ms for right-sided PVCs,  $P<0.001$ ). Nevertheless, the median distance between the AUT-EAS and MAN-EAS was only 3.1 mm (0–6.4 mm), with 33/100 (33%) of the patients showing an inter-EAS distance <1 mm.

There were seven patients (7%) with an inter-EAS distance >10 mm. The distribution of SOO locations in these cases was: 3 LV, 2 RVOT, 1 LVOT, and 1 RV; despite an increased inter-EAS distance, the median distance between the e-RFp and the respective EAS was not significantly different between the AUT and MAN maps [12.3 (4.6–15.6) vs. 4.4 (2.6–10.2) mm, respectively;  $P=0.15$ ]. There was one case, assigned to the AUT-method, with an inter-EAS distance of



20 mm; it corresponded to a patient with non-ischaemic cardiomyopathy and peri-Hisian PVCs related to the presence of septal intramyocardial fibrosis. The AUT-method failed for some points due to wrong LAT annotation at atrial far-field signals.<sup>5</sup>

## Procedure and clinical outcomes

While fluoroscopy time, total number of RF applications, and RF time were similar for both groups, significantly more activation points at the activation maps were acquired in the AUT-arm (Table 2). On the other hand, mapping and procedure times were significantly shorter for the AUT-arm when compared with the MAN-arm (Table 2).

Mapping success, as previously defined, was practically identical for both groups (62% AUT vs. 60% MAN;  $P = 0.84$ ). Acute procedure success was significantly better for the AUT-arm (100% vs. 88%;  $P = 0.01$ ), but without differences in clinical success during follow-up (92% AUT vs. 88% MAN;  $P = 0.51$ ). There were four patients in the AUT-arm who did not meet the criteria for early clinical success despite a successful procedure; two corresponded to PVCs arising from the LV summit, one from the RVOT, and one from the peri-Hisian region.

Mean PVC burden after the end of follow-up was  $2.9 \pm 5.1\%$ , representing a mean burden reduction of  $85 \pm 29\%$ , without differences between the AUT and MAN arms ( $P = 0.78$ ). No procedure-related complications were identified in any patient. Antiarrhythmic drugs were routinely discontinued after the procedure, except  $\beta$ -blockers for those patients (28/100, 28%) with prior structural heart disease.

## Discussion

### Main findings

To the best of our knowledge, this is the first multicentre randomized study assessing the possible benefits of a full-automated approach for PVC mapping (PVC-ECG recognition and LAT annotation) during PVC ablation procedures, as compared with a conventional, manual approach carried out by expert operators. The AUT-method

comprises two tools, WF annotation and an ECG pattern matching algorithm, already available in the CARTO3 electroanatomic navigation system. Although the primary endpoint of the study (mapping success as previously defined) was equally achieved using both approaches, the AUT-method was associated with a greater acute procedural success and similar clinical efficacy during follow-up, and allowed to perform more efficient procedures in terms of mapping density and procedure times, by permitting to acquire higher density maps in less time.

### Accuracy of bipolar- and unipolar-based local activation time annotation methods

The aspect that determines to a greater extent the results of catheter ablation of PVCs is the accuracy of LAT annotation during activation mapping. In this regard, the use of either B-EGM- or U-EGM-based annotations has some drawbacks. Briefly, the amplitude of B-EGMs is influenced by the underlying substrate, direction of WF propagation, bipole orientation, electrode size, and inter-electrode spacing.<sup>2,3</sup> Manual annotation of B-EGMs can be challenging, particularly in cases of low-voltage signals or in the presence of multiple components, a specially important aspect in LVOT-PVCs and fibrotic substrates.<sup>5,10</sup> The annotation at the onset of B-EGM<sup>11,12</sup> has the advantage of delimiting an unequivocal signal, but this method is still sensitive to far-field activation and may lead to less accurate activation maps.<sup>4,13</sup> As for U-EGMs, they contain significant far-field signal generated by depolarization of remote tissue; further on, the typical unipolar QS complex sought at the EAS in focal arrhythmias may be also recorded when the exploring electrode is not in sufficient contact with the underlying tissue.<sup>2</sup> Moreover, the type of U-EGM pattern registered may be also related to the size of the mapping catheter.<sup>14</sup>

In order to standardize the determination of LAT and improve the accuracy of activation maps, several algorithmic methods were developed by El Haddad *et al.*<sup>4</sup>; one of them, based on the maximal  $-dV/dt$  in the U-EGM<sup>15,16</sup> within the window demarcated by the B-EGM, reached the highest accuracy and was integrated as a ready-to-use tool into CARTO3 navigation system. The results of the present

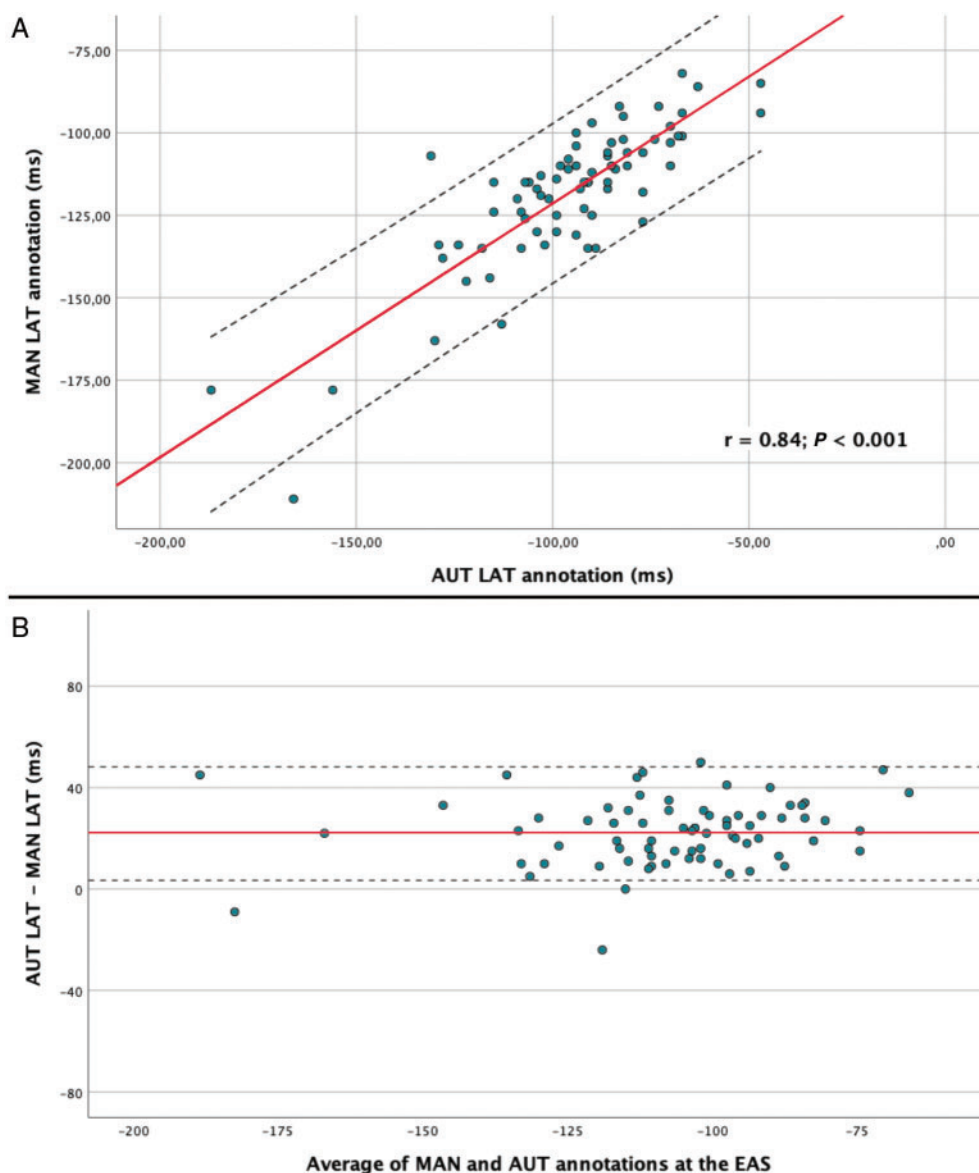


**Figure 5** (A) Correlation in LAT annotation at the EAS between the AUT and MAN-methods. (B) Bland–Altman plot showing agreement between automatic and manual LAT annotations at the EAS identified. AUT, automatic; EAS, earliest activation site; LAT, local activation time; MAN, manual.

randomized study evaluating this tool permit to assess the potential clinical benefit of the use of this algorithmic method, which we have referred to as WF method.

### Utility of a full-automatic local activation time annotation system during premature ventricular complex ablation procedures

The proposed automatic LAT annotation approach, named AUT-method, was not only based on WF annotation, as previously discussed, but in its integration with an ECG pattern matching algorithm to automatize the whole process of activation mapping. This last

algorithm allows to automatically annotate LAT each time the system detects a PVC which is concordant to a previously acquired PVC-ECG reference, after setting a minimum percentage of correlation in the 12-lead surface ECG. In this study, the lowest correlation was manually set at 98%, thus avoiding wrong annotation of ventricular complexes other than the clinical PVC, such as those resulting from inadvertent topo-stimulation with the mapping catheter.

Annotation of WF has previously shown<sup>4,5</sup> to underestimate LAT, in the sense that systematic delayed annotations are noted when compared with manual annotation, particularly in cases of LVOT-PVCs. This has been related to the frequent presence of presystolic bipolar potentials in this area,<sup>17</sup> which correspond to myocardial extensions into the aortic root.<sup>18</sup> In this regard, other studies have

**Table 2** Total mapping time, number of RF applications, RF time, and procedure time

	Total (n = 100)	MAN-method (n = 50)	AUT-method (n = 50)	P-value
Mapping time (min)	29.1 ± 13.9	32.8 ± 12.6	25.5 ± 14.3	0.009*
Total acquired points	103 (67–165)	79 (52–111)	136 (94–222)	<0.001*
SOO acquired points	80 (51–135)	60 (35–80)	120 (81–188)	<0.001*
No. of RF applications	2 (2–4)	2 (2–4)	2 (2–4)	0.91
RF time (s)	90 (60–161)	90 (53–188)	90 (62–151)	0.86
Fluoroscopy time (min)	4.2 ± 2.9	4.4 ± 3.2	3.9 ± 2.6	0.39
Procedure time (min)	61.1 ± 25.7	67.4 ± 25.2	54.8 ± 24.8	0.014*

AUT, automatic; MAN, manual; RF, radiofrequency; SOO, Site of origin.

\*Statistically significant differences ( $P < 0.05$ ).

shown that low, fractionated B-EGM signals may be found during sinus rhythm at the SOO areas, at least in the RVOT, which may be related to diseased myocardial tissue from which PVC arise.<sup>19</sup> However, since the annotation delay using WF is systematic, it has been also shown<sup>5</sup> that, in terms of accuracy in the SOO identification, the effective RF point was equally well identified either using WF or manual annotation of B-EGM onset. Far beyond these technical aspects, thoroughly reviewed in previous studies, this multicentre randomized study demonstrates that the full automatization of activation mapping during PVC ablation procedures is feasible in the clinical practice, while being more efficient than conventional, manual mapping.

## Study limitations

The results of this study cannot be applied to arrhythmia mechanisms other than focal, when using multi-electrode or mini-electrode catheters to create activation maps, or when using different navigation systems. Contact-force sensing technology was not systematically used; therefore, its influence on automatic annotation cannot be determined. One of the limiting aspects of WF annotation refers to the need to adjust the window of interest at the end of the QRS to avoid the detection of far-field atrial signals; despite this, the presence of wrong annotated points cannot be fully excluded. On the other hand, an automatic LAT annotation approach critically depends on the quality of the unipolar signals; noisy signals (i.e. due to external interferences) may cause obtention of misleading activation maps. Finally, the unavailability of 12-lead Holter monitors was a limitation when attributing recurrences to the reappearance of the original PVC.

## Conclusions

During PVC ablation procedures, a full-automatic activation mapping method that uses an ECG pattern matching algorithm plus WF annotation of LAT is feasible, reaching similar mapping success and clinical outcomes when compared with a conventional, manual approach carried out by expert operators. Automatic activation mapping is more efficient in terms of mapping and procedure times, while allowing the acquisition of higher density maps.

## Funding

This study was funded by Investigator-Initiated Study Grant IIS494 from Biosense Webster, Inc. ClinicalTrials.gov Identifier: NCT03340922.

**Conflict of interest:** D. S. is an employee of Biosense Webster, Inc. A.B. has received research funding and lecturing honoraria from Biosense Webster, Inc. The other authors have no other relevant affiliations or financial involvement with any organization or entity with a financial conflict with the subject matter or materials discussed in the manuscript apart from those disclosed.

## Data availability

The data that support the findings of this study are available from the corresponding author (A.B.) upon reasonable request.

## References

1. Cronin EM, Bogun FM, Maury P, Peichl P, Chen M, Namboodiri N *et al*. 2019 HRS/EHRA/APHS/LAHS expert consensus statement on catheter ablation of ventricular arrhythmias. *Europace* 2019;**21**:1143–4.
2. Stevenson WG, Soejima K. Recording techniques for clinical electrophysiology. *J Cardiovasc Electrophysiol* 2005;**16**:1017–22.
3. Ndrepepa G, Caref EB, Yin H, El-Sherif N, Restivo M. Activation time determination by high-resolution unipolar and bipolar extracellular electrograms in the canine heart. *J Cardiovasc Electrophysiol* 1995;**6**:174–88.
4. El Haddad M, Houben R, Stroobandt R, Van Heuverswyn F, Tavernier R, Duytschaever M. Novel algorithmic methods in mapping of atrial and ventricular tachycardia. *Circ Arrhythm Electrophysiol* 2014;**7**:463–72.
5. Acosta J, Soto-Iglesias D, Fernández-Armenta J, Frutos-López M, Jáuregui B, Arana-Rueda E *et al*. Clinical validation of automatic local activation time annotation during focal premature ventricular complex ablation procedures. *Europace* 2018;**20**:f171–8.
6. Baser K, Bas HD, Yokokawa M, Latchamsetty R, Morady F, Bogun F. Infrequent intraprocedural premature ventricular complexes: implications for ablation outcome. *J Cardiovasc Electrophysiol* 2014;**25**:1088–92.
7. Andreu D, Berrueto A, Fernández-Armenta J, Herczku C, Borràs R, Ortiz-Pérez JT *et al*. Displacement of the target ablation site and ventricles during premature ventricular contractions: relevance for radiofrequency catheter ablation. *Heart Rhythm* 2012;**9**:1050–7.
8. Penela D, Van Huls Vans Taxis C, Aguinaga L, Fernández-Armenta J, Mont L, Castel MA *et al*. Neurohormonal, structural, and functional recovery pattern after premature ventricular complex ablation is independent of structural heart disease status in patients with depressed left ventricular ejection fraction: a prospective multicenter study. *J Am Coll Cardiol* 2013;**62**:1195–202.
9. Penela D, De Riva M, Herczku C, Catto V, Pala S, Fernández-Armenta J *et al*. An easy-to-use, operator-independent, clinical model to predict the left vs. right ventricular outflow tract origin of ventricular arrhythmias. *Europace* 2015;**17**:1122–8.

10. Alcaine A, Soto-Iglesias D, Calvo M, Guiu E, Andreu D, Fernández-Armenta J et al. A wavelet-based electrogram onset delineator for automatic ventricular activation mapping. *IEEE Trans Biomed Eng* 2014;**61**:2830–9.
11. Gallagher JJ, Kasell J, Sealy WC, Pritchett EL, Wallace AG. Epicardial mapping in the Wolff–Parkinson–White syndrome. *Circulation* 1978;**57**:854–66.
12. Gallagher JJ, Kasell JH, Cox JL, Smith WM, Ideker RE, Smith WM. Techniques of intraoperative electrophysiologic mapping. *Am J Cardiol* 1982;**49**:221–40.
13. Paul T, Moak JP, Morris C, Garson A. Epicardial mapping: how to measure local activation? *Pacing Clin Electrophysiol* 1990;**13**:285–92.
14. Liu M, Jiang J, Su C, Li J, Chen X, Ma Y et al. Electrophysiological characteristics of the earliest activation site in idiopathic right ventricular outflow tract arrhythmias under mini-electrode mapping. *J Cardiovasc Electrophysiol* 2019;**30**: 642–50.
15. Ideker RE, Smith WM, Blanchard SM, Reiser SL, Simpson EV, Wolf PD et al. The assumptions of isochronal cardiac mapping. *Pacing Clin Electrophysiol* 1989;**12**: 456–78.
16. Delacretaz E, Soejima K, Gottipaty VK, Brunckhorst CB, Friedman PL, Stevenson WG. Single catheter determination of local electrogram prematurity using simultaneous unipolar and bipolar recordings to replace the surface ECG as a timing reference. *Pacing Clin Electrophysiol* 2001;**24**:441–9.
17. Ouyang F, Fotuhi P, Ho SY, Hebe J, Volkmer M, Goya M et al. Repetitive monomorphic ventricular tachycardia originating from the aortic sinus cusp: electrocardiographic characterization for guiding catheter ablation. *J Am Coll Cardiol* 2002;**39**:500–8.
18. Gami AS, Noheria A, Lachman N, Edwards WD, Friedman PA, Talreja D et al. Anatomical correlates relevant to ablation above the semilunar valves for the cardiac electrophysiologist: a study of 603 hearts. *J Interv Card Electrophysiol* 2011; **30**:5–15.
19. Letsas KP, Efremidis M, Vlachos K, Asvestas D, Takigawa M, Bazoukis G et al. Right ventricular outflow tract low-voltage areas identify the site of origin of idiopathic ventricular arrhythmias: a high-density mapping study. *J Cardiovasc Electrophysiol* 2019;**30**:2362–9.